Available online at www.sciencedirect.com
SCIENCE DIRECT®
Journal of Photochemistry and Photobiology A: Chemistry 165 (2004) 91–96
Journal of Photochemistry and Photobiology A:Chemistry
www.elsevier.com/locate/jphotochem

Neural computation to predict TiO_2 photocatalytic efficiency for nitrogen oxides removal

Filofteia-Laura Toma, Sofiane Guessasma*, Didier Klein, Ghislain Montavon, Ghislaine Bertrand, Christian Coddet

LERMPS—UTBM, Site de Sévenans, Rue Leupe, 90010 Belfort Cedex, France

Received 12 February 2004; received in revised form 12 February 2004; accepted 2 March 2004

Abstract

An artificial neural network (ANN) was built to analyze the decrease of nitrogen oxides relative to TiO_2 powder photocatalytic efficiency. Experimental sets were considered to train and test ANN where it was possible to identify an optimized structure representing the correlations between experimental variables and NO and NO_x efficiencies. Predicted results permitted to point out the role of exposed surface and powder mass.

Keywords: Artificial neural network; Photocatalysis; TiO_2; Nitrogen oxides removal

1. Introduction

The photocatalysis is a technique that allows environmental purification of air and water by decomposition and removal of harmful gases. Titanium dioxide is one of the most important photocatalyst used for such applications. Light excitation of TiO_2 semiconductor, under a wavelength between 360 and 380 nm, generates electrons and holes in the conduction and valence bands, respectively. These species are very reactive and can either recombine or diffuse to semiconductor surface where they are trapped by adsorbed molecules of water and oxygen. They provoke the formation of hydroxyl radicals that attack pollutant molecules and thus degrade them.

TiO_2 photocatalytic efficiency depends on various parameters such as crystalline phase type, surface morphology, specific surface area and thermal treatment [1–4].

This paper deals with the decrease of nitrogen oxides concentration using the photocatalysis method over TiO_2 powders. The nitrogen oxides NO_x (especially NO and NO_2) forming by cars traffic, combustion of coals, thermal power plants participate in the formation of acid rain, greenhouse effect, photochemical pollution and major problems on the human health.

The aim of the present paper is to assess the possibility to predict photocatalytic activity of the titanium dioxide powder regarding the NO_x removal by the technique of neural computational method. In order to process large data generated by nitrogen oxides removal set up and to identify the role of experimental variables, an artificial neural network was built.

Such technique encodes relationships between process variables organized as inputs and outputs [5]. It permits also to take into account parameter interdependencies and process variability [6]. In this study, it is used to quantify the relationships between photocatalysis experiment variables namely TiO_2 powder mass, exposed surface and output variables, namely NO and NO_x efficiencies.

2. Procedure

2.1. Materials and experimental design

TiO_2 Degussa P25 (from Degussa AG) powder, generally considered as a reference in the photocatalytic tests, was used to evaluate the photocatalytic decrease of nitrogen oxides. The powder has a specific surface area of about 50 m^2/g (BET method, nitrogen adsorption at 77 K) and contains two crystalline phases: anatase (80 vol.%) and rutile. The powder contains spherical nanoparticles, with a diameter size between 15 and 25 nm (Fig. 1).

* Corresponding author. Tel.: +33-3-84-58-31-29; fax: +33-3-84-58-32-86.
E-mail address: sofiane.guessasma@utbm.fr (S. Guessasma).

1010-6030/$ – see front matter © 2004 Elsevier B.V. All rights reserved.
doi:10.1016/j.jphotochem.2004.03.004

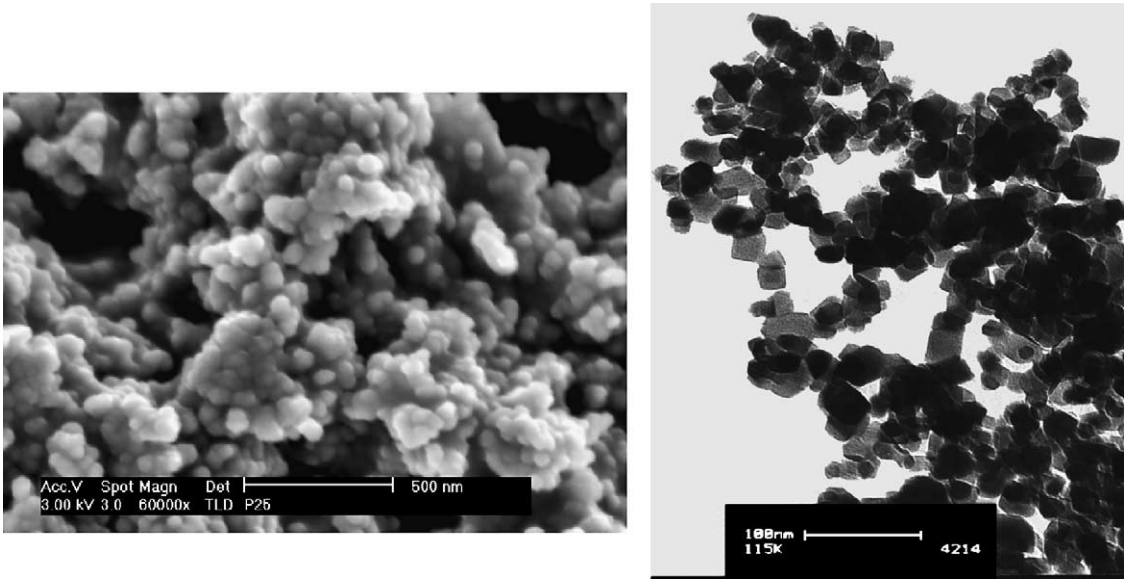

Fig. 1. Morphology of TiO_2 powder (Degussa P25) under SEM (left) and TEM (right) analysis.

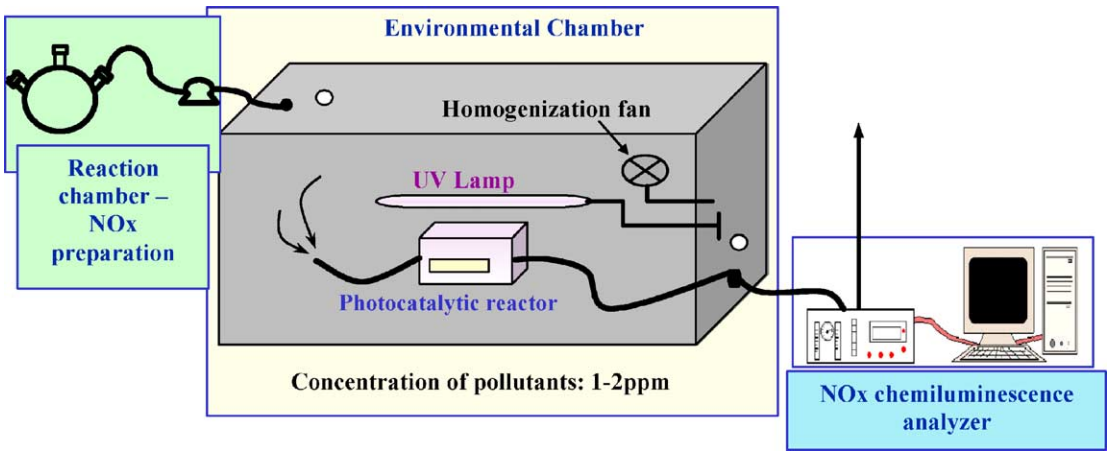

Fig. 2. Photocatalytic test chamber for nitrogen oxides removal.

The experimental set-up for NO_x photocatalytic removal described in a previous paper [7] is presented in Fig. 2. The nitrogen oxides, prepared in situ by chemical reaction between copper powder and nitric acid, were introduced in an environmental chamber (volume of about 0.4 m^3) allowing nitrogen oxides volume concentration of about 1.0–1.5 ppm. The photocatalytic reactor (100 mm × 100 mm × 5 mm) was equipped with a plexiglass window which allowed the light passage from an ultraviolet lamp (30% UVA and 4% UVB). This reactor was placed inside the environmental chamber and crossed by the NO_x flow. Nitrogen oxides amount was measured continuously using an AC-30M NO_x dual chamber chemiluminescence analyzer (Environmental SA, France) and recorded with an acquisition data system.

Before performing the photocatalytic test, a blank test was carried out without the photocatalyst. No significant changes in the nitrogen oxides concentrations were observed when the ultraviolet lamp was turned on. When Degussa P25 powder was used, variations in the nitrogen oxides were observed during the irradiation. During the photocatalytic test, a rapid decrease of the pollutants concentrations took place in the first minutes; after that this decrease became slower in time. When the lamp was turned off, the concentration of nitrogen oxides started to increase. The decrease of pollutant concentrations was obtained only in presence of both photocatalyst and ultraviolet light (Fig. 3).

The photocatalytic efficiency was evaluated after the 10 first minutes of UV irradiation, as the ratio of the removed concentration of nitrogen oxides. The decreases of pollutant concentrations, called efficiencies, were determined by the following relationships:

$$[NO]_{removed}\,(\%) = \frac{[NO]_{initial} - [NO]_{UV}}{[NO]_{initial}} \times 100 \qquad (1a)$$

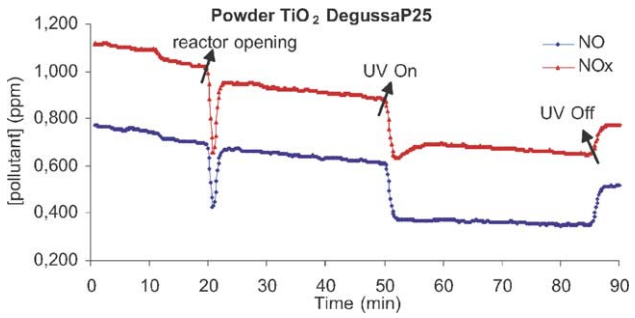

Fig. 3. Experimental photocatalytic test result over TiO_2 powder (Degussa P25).

Table 1
Parameters of photocatalytic tests

Number of test	Exposed surface (cm^2)	Powder quantity (g)
1	20	0.01
2		0.025
3		0.05
4		0.08
5	54	0.01
6		0.025
7		0.05
8		0.08

$$[NO_x]_{removed}\,(\%) = \frac{[NO_x]_{initial} - [NO_x]_{UV}}{[NO_x]_{initial}} \times 100 \qquad (1b)$$

where $[NO]_{removed}(\%)$ and $[NO_x]_{removed}(\%)$ are the concentration decreases of NO and NO_x, respectively, in the presence of the catalyst and UV irradiation; $[NO]_{initial}$ and $[NO_x]_{initial}$ represent the values of the NO and NO_x concentrations without irradiation; $[NO]_{UV}$ and $[NO_x]_{UV}$ are the values of the NO and NO_x concentrations under UV irradiation.

The photocatalytic tests were performed over different powder quantities of Degussa P25, ranging from 0.01 to 0.08 g, to observe the variations in the photocatalytic diminution of nitrogen oxides. The catalyst was exposed to UV over two circular surfaces of 20 and around 54 cm^2, respectively. The parameters of photocatalytic tests are resumed in Table 1.

2.2. Neural computation

An ANN was built to relate powder mass, exposed surface and time to NO and NO_x efficiencies. Such structure encodes the relationships between I/O variables through a large set of neurons which acts as mathematical decision centers. These are connected by weights which are numbers translating the strength of neuron connections. Input variables are looked as number fluxes which feed the network structure and reach the output pattern. ANN optimization process is based on a training procedure to decrease the error between ANN response and experimental response for a given set of input variables. Such optimization considers neuron number and weight updates. Optimization parameters are summarized in Table 2. In this study, 488 experimental sets are used to feed an ANN structure. The network input contained three neurons representing powder quantity, exposure time and surface, respectively. The output pattern comprised two neurons representing the photocatalytic response, namely NO and NO_x efficiencies.

Experimental sets are organized in training and test samples. The first category was used to tune neuron network weights and the second category to test the network configuration. Neuron penalty is introduced to optimize neuron number. A stopping criterion was applied corresponding to a fixed number of training and test cycles: 2000 cycles were achieved for each network configuration after approximately 1 h of computation time.

Table 2
ANN optimization parameters

Parameter	Value	Comments		
		Variable type	Minimum	Maximum
Input variables	3	Exposed surface (cm^2)	0 for 20	1 for 54
		Exposed time (min)	0	10
		Powder mass (g)	0	0.1
Output variables	2	NO efficiency (%)	0	100
		NO_x efficiency (%)	0	100
Architecture	Feed-forward	See [6] for definition		
Training algorithm	Quick propagation	See [5] for definition		
		Category	Sample number	
Database	488 samples	Train	244	
		Test	244	
Optimization cycle number	2000	One cycle corresponds to training and testing of the whole database passage		
Number of hidden layers	3	Suitable for non linear correlations. See [5] for further comments		
Number of neurons in each layer	Varied	This number is calculated from the optimization procedure		

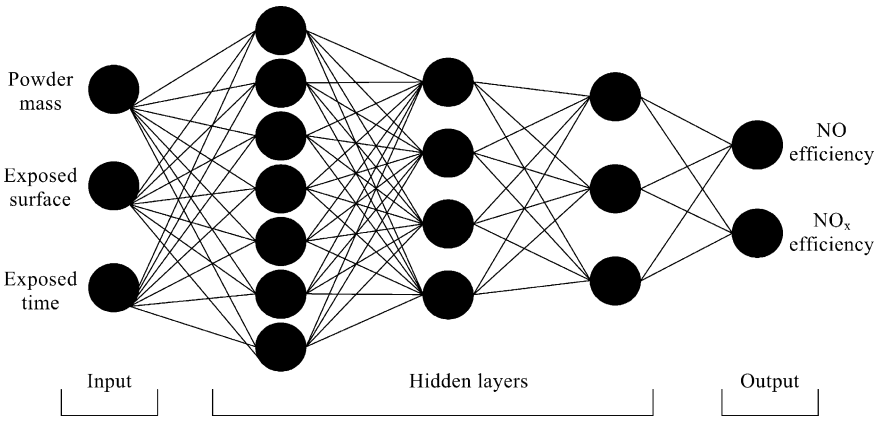

Fig. 4. ANN optimized structure.

3. Results and discussion

Fig. 4 shows the optimized ANN structure characterized by three hidden layers containing seven, four and three neurons, respectively. Correlations were learnt from the database with a percentage of 98.57%. The overall optimization error was in the average less than 5%. With the optimized structure, it was possible to quantify the effect of each experiment variable by varying independently each of them and collecting NO and NO_x efficiencies.

Figs. 5 and 6 present the predicted photocatalytic efficiency of the Degussa P25 powder for the diminution of nitrogen oxides, function of powder quantity and exposed surface to ultraviolet irradiation.

In all cases, it was observed that a fast diminution in the nitrogen oxides concentration was recorded in the first min-

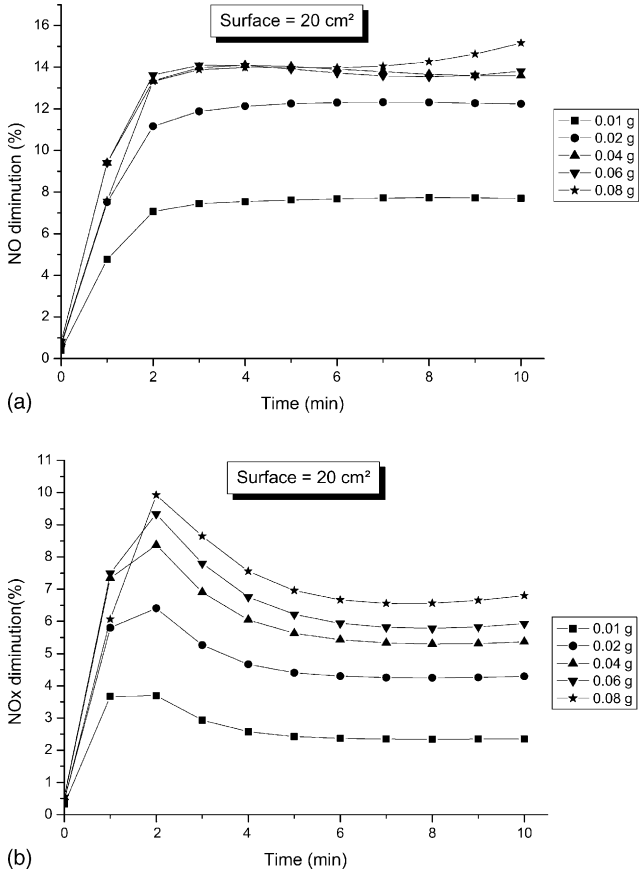

Fig. 5. ANN predicted curve of (a) NO and (b) NO_x temporal decrease for different powder quantities (exposed surface = 20 cm^2).

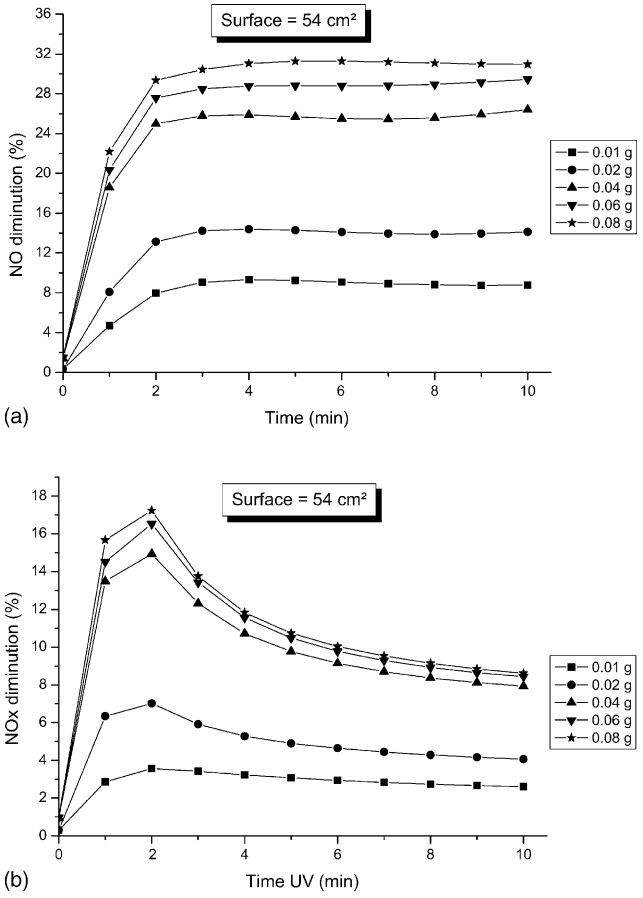

Fig. 6. ANN predicted curve of (a) NO and (b) NO_x temporal decrease for different powder quantities (exposed surface = 54 cm^2).

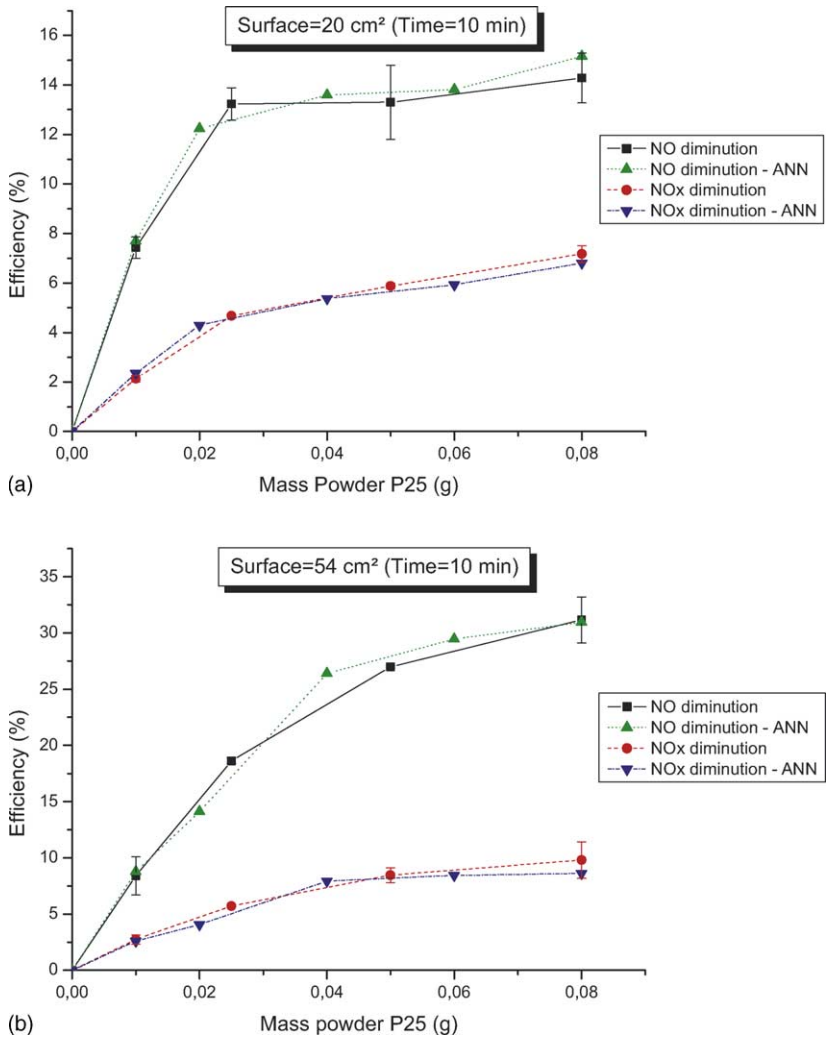

Fig. 7. Comparison between experimental and simulated photocatalytic results for surface of (a) 20 cm^2 and (b) 54 cm^2. Results obtained after 10 min of ultraviolet irradiation.

utes of illumination. Then, this diminution remained almost constant with UV time for the NO and was slowly decreased for NO_x pollutant. When the powder was spread out over the surface of 20 cm^2, NO diminution varied with the P25 quantity from 7 to 15% after 10 min of UV illumination. In the meantime, NO_x diminution is predicted to be around 3–7% when the mass increased from 0.01 to 0.08 g (Fig. 5).

For an exposed surface of 54 cm^2 (Fig. 6), simulation results show that NO removal was between 8% (for 0.01 g) and 31% (for 0.08 g) and NO_x decrease varied from 3 to 10% with powder mass (Fig. 6). When experimental photocatalytic tests were carried out over the powder exposed on the surface of 54 cm^2, NO removal increased from 8% (0.01 g powder) to 32% (0.08 g P25), whereas NO_x removal varied from 4 to 14% after 10 min of ultraviolet irradiation.

These results show overly that photocatalytic efficiency of Degussa P25 was higher when powder was exposed to illumination onto a larger surface. Moreover, for a given exposed surface, efficiency increased with powder mass until an optimal value over which efficiency remained practically the same. Zhang et al. [8] and Herrmann [9] quoted also that photocatalytic degradation rate of different aqueous pollutants increased with a catalyst mass until a maximum value that depended on the type of photocatalyst, the photoreactor geometry and working conditions. The mass limit corresponded to the case where all TiO_2 particles (i.e. the whole exposed surface) were irradiated and participated to the photocatalytic process. For higher powder quantities, a screening effect of particles in excess occurs, which masks a part of the photoactive surface. In such a way, Byrne et al. [10] noted that photocatalytic efficiency of the TiO_2 in the degradation of phenol concentration seemed decrease with the mass of the photocatalyst.

In addition, optimal powder mass depended on the exposed surface to ultraviolet irradiation. In this study, the limit value was 0.06 g for a surface of 20 cm^2 and 0.08 g for a surface of 54 cm^2.

Fig. 7 compares results obtained from the photocatalytic tests with those obtained from neural computation after the

10 min of ultraviolet irradiation. A good agreement between data was obtained with a standard deviation less than 4% for both exposed surfaces. Moreover, it was possible to obtain intermediate predicted points that were not considered in photocatalysis experiments. These last ones were not far from the interpolation curves.

4. Conclusion

The use of ANN as statistical tool permitted to predict the photocatalytic removal of nitrogen oxides (NO and NO_x) over a TiO_2 powder. Predicted results were in good agreement with experiments and showed a significant increase of efficiency when powder mass and exposed surface increased. A limiting mass was identified which depended on the exposed surface over which efficiency increase was not possible for both exposed surfaces. Experiments with powder mass larger than 0.1 g will be considered in a future work to verify the stability of NO and NO_x efficiencies.

Acknowledgements

One of authors (F.L. Toma) would like to thank to Dr. D. Robert (Laboratoire de Chimie et Applications “Procédés Propres et Environnement”, Université de Metz, France) for scientific discussions and delivery of TiO_2 Degussa P25 powder and to Dr. S. Bégin—Colin (Laboratoire de Sciences et Génie des Matériaux et de Métallurgie, UMR CNRS 7584, Ecole des Mines de Nancy) for carrying out the SEM/TEM powder analysis.

References

[1] H. Gerisher, Conditions for an efficient photocatalytic activity of TiO_2 particles, in: D.F. Ollis, H. Al-Ekabi (Eds.), Proceedings of the Photocatalytic Purification and Treatment of Water and Air, Elsevier, Amsterdam, 1993, pp. 1–17.

[2] K. Tanaka, T. Hisanaga, A.P. Rivera, Effect of crystal form of TiO_2 on the photocatalytic degradation of pollutants, in: D.F. Ollis, H. Al-Ekabi (Eds.), Proceedings of the Photocatalytic Purification and Treatment of Water and Air, Elsevier, Amsterdam, 1993, pp. 169–178.

[3] N. Negiski, K. Takeuchi, T. Ibusuki, The surface structure of titanium dioxide thin film photocatalyst, Appl. Surf. Sci. 121/122 (1997) 417–420.

[4] K. Hashimoto, K. Wasada, N. Toukai, H. Komonami, Y. Kera, Photocatalytic oxidation of nitrogen monoxide over titanium(IV) oxide nanocrystals large size areas, J. Photochem. Photobiol. A: Chem. 136 (2000) 103–109.

[5] S. Guessasma, G. Montavon, C. Coddet, On the neural network concept to describe the thermal spray deposition process: an introduction, in: E. Lugscheider (Ed.), Proceedings of the International Thermal Spray Conference 2002, DVS-Verlag/GmbH, Düsseldorf, Germany, 2002, pp. 435–439.

[6] S. Guessasma, G. Montavon, C. Coddet, Modeling of the APS plasma spray process using artificial neural networks: basic, J. Comput. Mater. Sci. 29 (2004) 315–333.

[7] F.L. Toma, N. Berger-Keller, G. Bertrand, D. Klein, C. Coddet, Photocatalytic properties of TiO_2 coatings as a function of coating and substrate characteristics, in: C. Moreau, B. Marple (Ed.), Thermal Spray 2003: Advancing the Science and Applying the Technology, ASM International, Materials Park, OH, USA, 2003, pp. 1331–1335.

[8] Y. Zhang, J.C. Crittenden, D.W. Hand, D.L. Perram, Fixed-bed photocatalysts for solar decontamination of water, Environ. Sci. Technol. 28 (1994) 435–442.

[9] J.-M. Herrmann, Heterogeneous photocatalysis: fundamentals and applications to the removal of various types of aqueous pollutants, Catal. Today 53 (1999) 115–129.

[10] J.A. Byrne, B.R. Eggins, N.M.D. Brown, B. McKinney, M. Rouse, Immobilisation of TiO_2 powder for the treatment of polluted water, Appl. Catal. B: Environ. 17 (1998) 25–36.